ESTIMATION OF THE LOCAL INCIDENCE ANGLE MAP FROM A SINGLE SAR IMAGE

Gerardo Di Martino [(1)], Alessio Di Simone [(1)], Antonio Iodice [(1)], Daniele Riccio [(1)], Giuseppe Ruello [(1)]

[(1)] University of Naples Federico II, Via Claudio 21, 80125, Naples, Italy, Email: {gerardo.dimartino, alessio.disimone, antonio.iodice, daniele.riccio, giuseppe.ruello}@unina.it

ABSTRACT

The ongoing ESA SENTINEL-1 mission witnesses the key role of synthetic aperture radar (SAR) systems in Earth observation and monitoring by means of a continuous radar mapping of our planet's surface. By exploiting the peculiarities of the radiation-matter interaction, SAR data contain huge information concerning the physical and chemical properties of the illuminated surface. Due to the huge number of surface parameters influencing SAR data formation, very few scientific papers concern the estimation of such parameters directly from a single SAR image. In this paper, a technique aimed at the estimation of the local incidence angle map from a single SAR image is derived. The proposed method relies on a solid theoretical background and well-assessed models and methods. The efficacy of the new estimation technique is assessed with both simulated and actual SAR images.

1. INTRODUCTION

For the last two decades, synthetic aperture radar (SAR) imagery has become a fundamental tool for natural resources monitoring and environmental hazards management and control. The ongoing ESA SENTINEL-1 mission witnesses the increasing interest in SAR sensors thanks to their relative insensitivity to weather conditions and solar illumination. However, as demonstrated by the recent Huygens-Cassini mission to Saturn and its moons and the ESA planned JUICE (Jupiter Icy Moons Explorer) mission, SAR sensors and imagery are an essential tool even for analysis of other celestial bodies [1]. In the latter context, one of the most important issue is the possibility to obtain a first (rough) estimation of the topography, namely a Digital Elevation Model (DEM) of the surface. Although rough DEMs exist for most of the Earth's surface, e.g. those provided by the SRTM mission, SAR imagery can be still exploited to estimate higher resolution DEMs thanks to the (sub-)meter resolution of recent SAR sensors. Very high-resolution DEMs provided with lidar data are still limited.

In the last decades, several techniques aimed at estimating the local topography of the sensed surface have been developed, namely stereoscopy [2], [3], shape from shading (SfS) (or radarclinometry) [4]-[6], polarimetry [7], interferometry [8]. At variance with other methods, the SfS approach presents the very interesting feature of requiring only a single SAR image, thus requiring a much simpler system architecture and image acquisition process, key features in planning space missions. However, a vague feeling of scepticism accompanies application of SfS techniques on SAR images. SfS is nicely valued if optical images are in order; but within the radar community (which also terms it, radarclinometry) SfS is commonly considered impracticable. This impracticability is partially due to the use of inadequate models describing electromagnetic scattering from a natural scenario, as the Lambertian model commonly used in the radarclinometry community. In addition, the complexity of the SfS problem can be significantly reduced considering the problem of the local incidence angle estimation instead of the local height estimation. An accurate inversion procedure aimed at retrieving the local incidence angle map is a necessary step to a reliable DEM estimation via the SfS approach. It is worth to note that an adequate modelling of the SAR image is required. In the existing literature, there is a general lack of algorithms allowing for the estimation of meaningful topographical parameters of natural surfaces from their radar image. This is due to the absence of a reliable direct model for microwave imaging of natural surfaces. In this paper we provide an inversion approach to the problem of local incidence angle estimation from a single SAR image of natural (terrestrial or not) landscapes. In particular, the proposed method is based on fractal electromagnetic and surface models, adequate to describe natural surfaces and corresponding electromagnetic scattering processes.

Besides the height retrieval problem, local incidence angle estimation has other, somehow surprising, applications, such as despeckling, as recently shown by the authors [9]-[11].

2. FORWARD (FRACTAL) MODEL

In order to derive a retrieval procedure suitable for SAR images of natural scenarios, a forward model linking SAR data to the parameters of interest (the local incidence angle in this case) is required. To this aim, we resort to the fractal geometry, since it represents the best and most suitable tool to describe the self-affinity and self-similarity features of natural surfaces. The forward model is then split in three parts: first, a model for natural surfaces is introduced; then a closed-form analytical model for electromagnetic scattering description is used to link the geometrical and

Proc. 'Living Planet Symposium 2016', Prague, Czech Republic, 9–13 May 2016 (ESA SP-740, August 2016)

electromagnetic surface parameters to the backscattering coefficient. Finally, a SAR image model relating the SAR intensity to the backscattering coefficient of the surface, and then to the surface parameters is introduced and described.

2.1. Surface Model

As shown in literature, the fractal geometry represents the best candidate to describe the irregularity and the roughness of natural scenes with a minimum number of parameters [12]-[15]. In this paper, the surface shape is modelled via a 2-D topological fractional Brownian motion (fBm) stochastic process, according to which:

$$\Pr\left\{z(x,y)-z(x',y')<\bar{\zeta}\right\}= \frac{1}{\sqrt{2\pi}s\tau^{H}}\int_{-\infty}^{\bar{\zeta}}\exp\left(-\frac{\zeta^{2}}{2s^{2}\tau^{2H}}\right)d\zeta \quad (1)$$

where Pr{} stands for "probability", $\bar{\zeta}$ is the considered height increment, $z(x,y)$ is the surface elevation, τ is the distance between the two considered points of coordinates (x,y) and (x',y'), and

- H: Hurst coefficient ($0 < H < 1$) related to the fractal dimension $D = 3-H$;
- T: topothesy [m], i.e., the distance over which chords joining points on the surface have a root mean square slope equal to unity.

2.2. Electromagnetic Scattering Model

The scattering behaviour of the surface is described via the Small Perturbation Method (SPM) suitable for fractal surfaces, that allows for both a closed-form and analytically tractable relationship between the surface parameters and the backscattering coefficient. According to this framework, the scattering behaviour of the surface reads as

$$\sigma_{mn}^{0}=2\pi 8k^{4}\cos^{4}\vartheta\left|\beta_{mn}\right|^{2}\frac{S_{0}}{\left(2k\sin\vartheta\right)^{2+2H}} \quad (2)$$

wherein k is the electromagnetic wavenumber of the incident field; S_0 is the spectral amplitude of the fBm surface; β_{mn} is a coefficient depending on transmitted and received signal polarization and the local incidence angle ϑ.

2.3 SAR Image Model

In this section, a model linking the SAR image intensity to the surface parameters is presented. The following model for the intensity SAR image I is used:

$$I = nG\Delta x\Delta r\sigma_{mn}^{0} \quad (3)$$

where n stands for speckle noise intensity, G is an absolute calibration constant, and Δx and Δr stand for the azimuth and slant range resolutions respectively. By substituting Eq. 2 in Eq. 3, the following model linking the noisy SAR image intensity to the surface parameters holds:

$$I = nG\Delta x\Delta r\pi\left(2k\right)^{2-2H}\cos^{4}\vartheta\left|\beta_{mn}\right|^{2}\frac{S_{0}}{\sin\vartheta^{2+2H}} \quad (4)$$

3. INVERSION PROCEDURE

Inversion of Eq. 4 requires the estimation of the absolute calibration constant G. A simple procedure can be set up once assumed that $<\vartheta>=\theta_0$, where $< >$ stands for the average over the entire image and θ_0 is the radar look angle. Consequently, G can be easily estimated as:

$$G=\frac{<I>}{a_{0}} \quad (5)$$

where $a_{0}=\Delta x\Delta r\pi\left(2k\right)^{2-2H}\cos^{4}\theta_{0}\left|\beta_{mn}\right|^{2}\frac{S_{0}}{\sin\theta_{0}^{2+2H}}$.

Once G is estimated, the incidence angle map can be retrieved by inverting Eq. 4. In order to reduce speckle effect, a despeckling preprocessing can be performed. Therefore, the following despeckled image is obtained:

$$I_{filt}=G\Delta x\Delta r2\pi 8k^{4}\cos^{4}\vartheta\left|\beta_{mn}\right|^{2}\frac{S_{0}}{\left(2k\sin\vartheta\right)^{2+2H}} \quad (6)$$

Inversion of Eq. (6) is performed as follows:

$$\hat{\vartheta}=\min_{\vartheta}\sum_{i,j}^{M,N}\left(I_{oss,i,j}-I_{filt,i,j}\left(\vartheta\right)\right)^{2} \quad (7)$$

To this aim, an estimation/knowledge of both sensor and surface parameters is required. Sensor parameters - spatial resolution, electromagnetic wavenumber, and radar look angle -, are assumed perfectly known, since they are provided together with the SAR image in the ancillary data. For what concerns surface parameters, the sensitivity analysis of the proposed scattering model provided in [10] shows that the backscattering coefficient in Eq. 2 is rather insensitive to the electromagnetic parameters – relative dielectric constant, and electrical conductivity – and topothesy. For such parameters, reference values for natural surfaces can be used. In presence of gentle topography, the Hurst coefficient plays a non-negligible role in SAR image formation. For this reason, it may be estimated via the algorithm in [13] directly from the SAR image. In the case of strict time requirements, typical values of H ($0.5 \leq H \leq 0.9$) can be used for the entire image without a significant performance degradation.

4. EXPERIMENTAL RESULTS

In this Section, a canonical fractal scenario is simulated to assess the performance of the proposed retrieval

procedure. In particular, we consider the fBm fractal surface in Fig. 1(c) with parameters $H = 0.8$, $T = 10^{-4}$m, relative dielectric constant $\varepsilon_r = 4$, and electrical conductivity $\sigma = 10^{-2}$S/m and simulate the corresponding single-look SAR image in Fig. 1(a) via the SARAS algorithm using the SPM option for scattering evaluation [16]. The SAR image is then pre-processed with a 5x5 spatial multilook in order to reduce speckle effects (Fig. 1(b)). The retrieved incidence angle map in Fig. 1(d) witnesses the efficacy of the technique both visually and quantitatively, as also demonstrated by the low error statistics. The incidence angle map is then accurately retrieved at all the image scales, since most topographic details are correctly estimated.

In Fig. 2, the algorithm is applied to a 2000x2000 single-polarized actual COSMO/SkyMed SAR image of the Vesuvio volcano acquired in stripmap configuration on August 3rd, 2011 in HH polarization (Fig. 2(a)). The despeckled image obtained applying the SARBM3D filter [17] and used for inversion purposes is shown in Fig. 2(b). In Fig. 2(c) the ground truth incidence angle map is shown. The outcome of the algorithm in Fig. 2(d) exhibits a satisfactory similarity with the ground truth map, as also indicated by the error statistics. A fixed value $H = 0.5$ is used in this scenario. The poorer performance with respect to the simulated case is due to the presence of vegetated areas, causing some mismatch between the proposed scattering model and the actual scattering behaviour of the surface. The incidence-angle independent volumetric scattering contribution of vegetation has been estimated and compensated via evaluation of the scattering in a very high incidence angle region on Mt Vesuvio. In addition, some geometrical distortions, such as layover and shadowing are clearly visible in correspondence of the crater and the ripples both in the reference and estimated maps.

5. CONCLUSIONS

In this paper, a procedure aimed at retrieving the local incidence angle from a single SAR image has been presented and described. The new algorithm relies on recent scattering and surface models based on the well-assessed fractal geometry. Besides some standard applications, which include DEM generation and refinement, other key applications, such as despeckling, could benefit from the proposed technique, as recently demonstrated by the authors [9]-[11].

6. REFERENCES

1. Grasset, O. et al. (2013). JUpiter ICy moons Explorer (JUICE): An ESA mission to orbit Ganymede and to characterise the Jupiter system. *Planet. Space Sci.* **78**, 1-21. doi:10.1016/j.pss.2012.12.002

2. Dhond, U.R. & Aggarwal, J.K. (1989). Structure from stereo – a review. *IEEE Trans. Syst., Man, Cybern.* **19**(6), 1489-1510. doi:10.1109/21.44067

3. Dowman, I., Pu-Huai, C., Clochez, O. & Saundercock, G. (1993). Heighting from stereoscopic ERS-1 data. In *Proc. 2nd ERS-1 Symp.*, 609-614.

4. Ostrov, D.N. (1999). Boundary Conditions and Fast Algorithms for Surface Reconstructions from Synthetic Aperture Radar Data. *IEEE Trans. Geosci. Remote Sens.* **37**(1), 335-346. doi: 10.1109/36.739066

5. Wildey, R.L. (1986). Radarclinometry for the Venus radar mapper. *Photogramm. Eng. Remote Sens.* **52**(1), 41-50.

6. Brooks, M.J. & Horn, B.K.P. (1989). *Shape From Shading*. Cambridge: MA: MIT Press.

7. Schuler, D.L., Lee, J.S. & De Grandi, G. (1996). Measurement of topography using polarimetric SAR images. *IEEE Trans. Geosci. Remote Sens.* **34**(5), 1266-1277. doi:10.1109/36.536542

8. Massonnet, D., & Rabaute, T. (1993). Radar interferometry: limits and potential. *IEEE Trans. Geosci. Remote Sens.* **31**(2), 455-464. doi: 10.1109/36.214922

9. Di Martino, G., Di Simone, A., Iodice, A., Riccio, D. & Ruello, G. (2015). Non-Local Means SAR Despeckling Based on Scattering. In *Proc. IEEE Int. Geosci. Remote Sens. Symp. (IGARSS' 15)*, Milan, Italy, 3172-3174. doi:10.1109/IGARSS.2015.7326491

10. Di Martino, G., Di Simone, A., Iodice, A. & Riccio, D. Scattering-Based Non-Local Means SAR Despeckling. *IEEE Trans. Geosci. Remote Sens.* **54**(6), 3574-3588. doi: 10.1109/TGRS.2016.2520309.

11. Di Martino, G., Di Simone, A., Iodice, A., Poggi, G., Riccio, D. & Verdoliva, L. Scattering-Based SARBM3D. *IEEE J. Sel. Topics Appl. Earth Observ. in Remote Sens.* (in press). doi: 10.1109/JSTARS.2016.2543303

12. Franceschetti, G., & Riccio, D. (2007). *Scattering, Natural Surfaces and Fractals*, Burlington: MA: Academic.

13. Di Martino, G., Riccio, D. & Zinno, I. (2012). SAR Imaging of Fractal Surfaces. *IEEE Trans. Geosci. Remote Sens.*, **50**(2), 630-644. doi:10.1109/TGRS.2011.2161997

14. Feder, J.S. (1988). *Fractals*, New York: Plenum Press.

15. Mandelbrot, B. (1983). *The Fractal Geometry of Nature*, New York: Freeman.

16. Franceschetti, G., Migliaccio, M., Riccio, D. & Schirinzi, G. (1992). SARAS: A SAR raw signal simulator. *IEEE Trans. Geosci. Remote Sens.*, **30**(1) 110-123. doi: 10.1109/36.124221

17. Parrilli, S., Poderico, M., Angelino, C.V. & Verdoliva, L. (2012). A nonlocal SAR image denoising algorithm based on LLMMSE wavelet shrinkage. *IEEE Trans. Geosci. Remote Sens.*, **50**(2) 606-616. doi: 10.1109/TGRS.2011.2161586

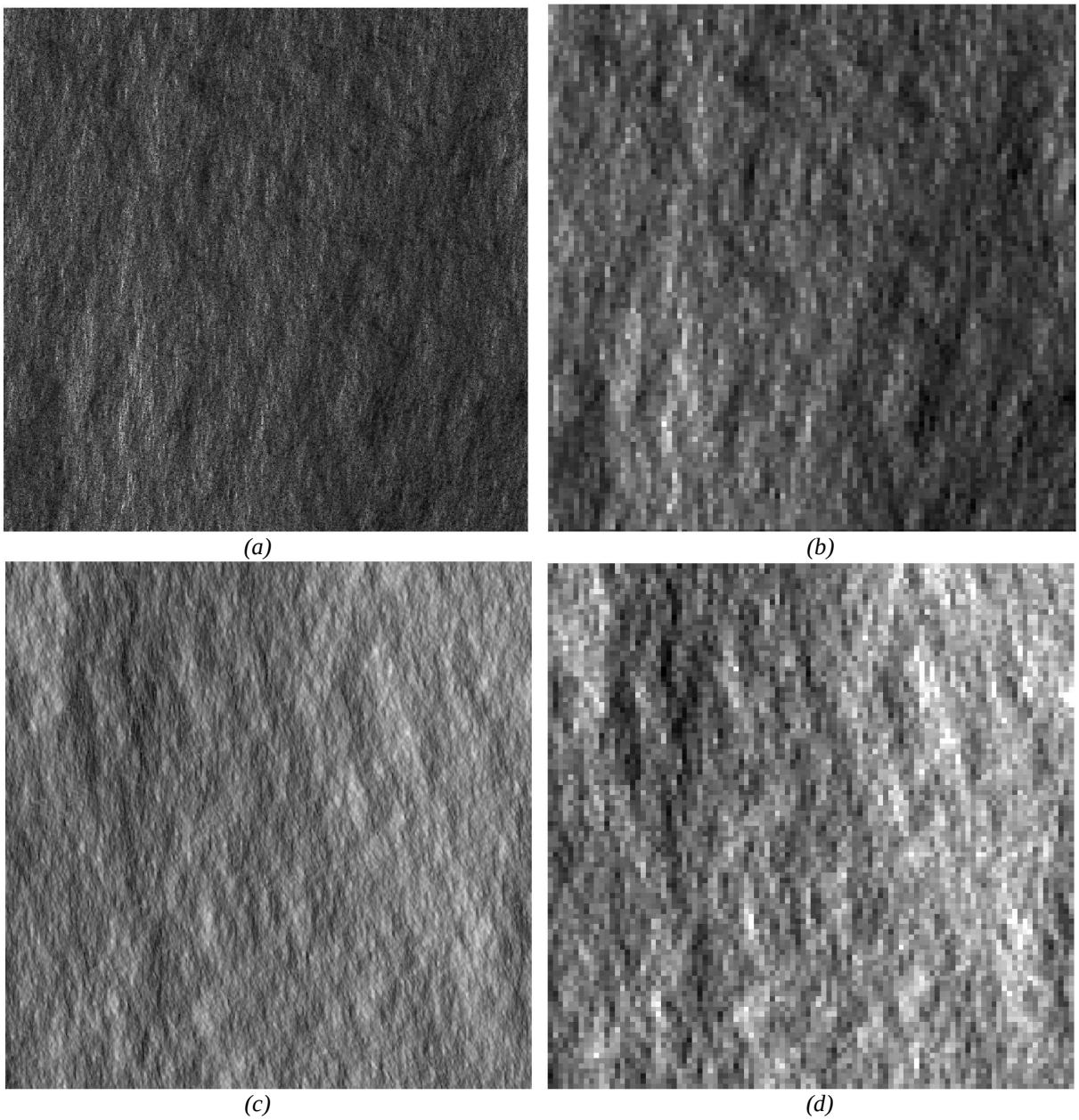

(a) *(b)* *(c)* *(d)*

Figure 1: Canonical case. (a) Single-look SAR image; (b) 5-look SAR image used as input; (c) ground truth incidence angle map in degrees; (d) incidence angle map estimated with the proposed technique shown with the same grayscale of the ground truth. Performance parameters in degrees: mean error = 1.59°. Median error = 1.76°. Standard deviation = 4.31°.

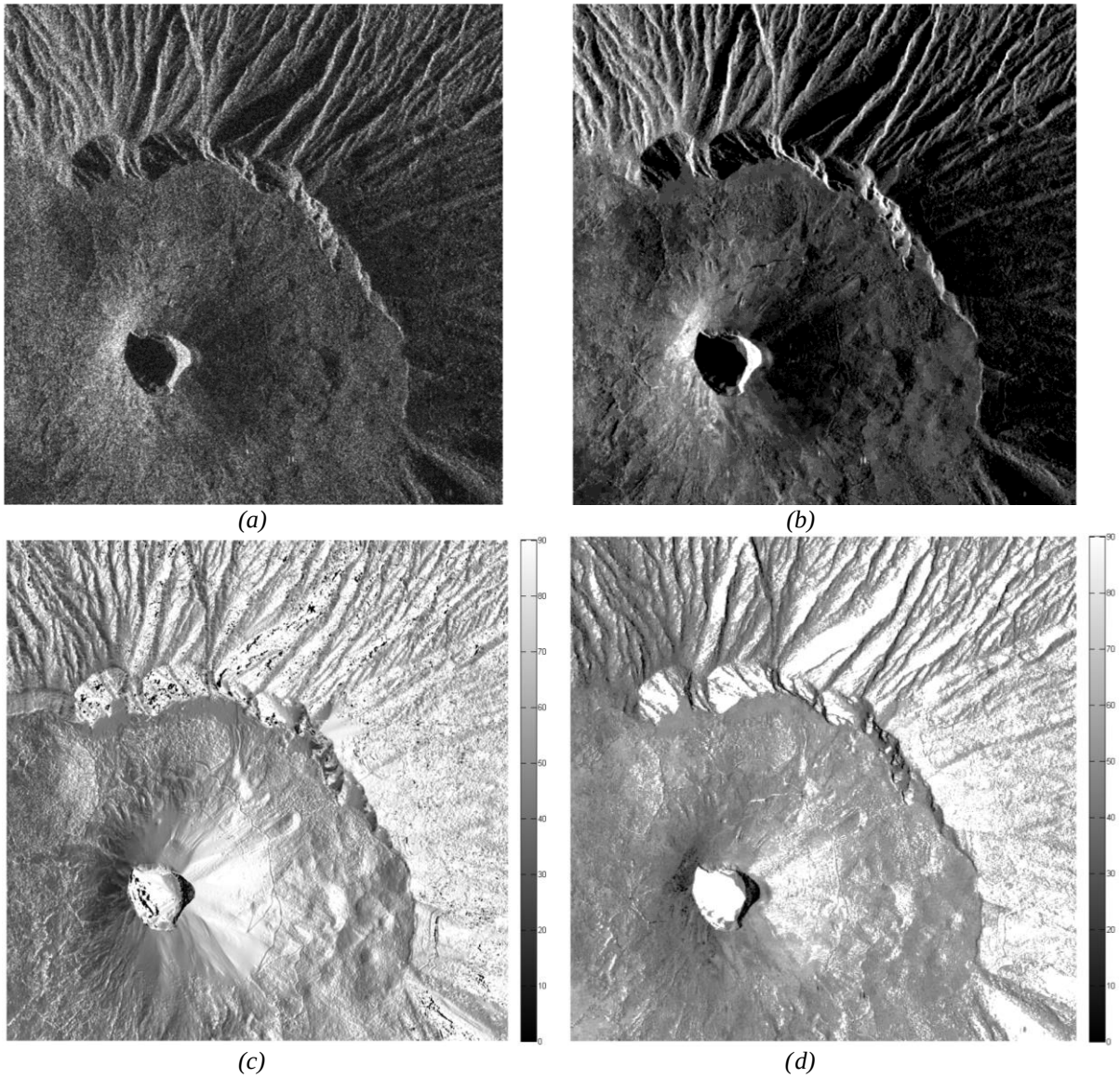

Figure 2: Actual case. (a) 2000x2000 single-look COSMO/SkyMed SAR image of the Vesuvius volcano acquired in stripmap configuration. (b) Despeckled SAR image used as input. (c) Ground truth incidence angle map in degrees derived from a lidar DEM. Strong geometrical distortions (layover and shadowing) cause some not-a-number points in the DEM projected in the SAR coordinate system. (d) Estimated local incidence angle map. Both the crater and the ripples are clearly visible. Performance parameters in degrees: mean error = 0.71°. Median error = 0.99°. Standard deviation = 14.52°.